DOI: 10.1534/genetics.104.026575

Clonal Mosaic Analysis of EMPTY PERICARP2 Reveals Nonredundant Functions of the Duplicated HEAT SHOCK FACTOR BINDING PROTEINs During Maize Shoot Development

Suneng Fu and Michael J. Scanlon[1]

Plant Biology Department, University of Georgia, Athens, Georgia 30602

Manuscript received January 16, 2004
Accepted for publication April 5, 2004

ABSTRACT

The paralogous maize proteins EMPTY PERICARP2 (EMP2) and HEAT SHOCK FACTOR BINDING PROTEIN2 (HSBP2) each contain a single recognizable motif: the coiled-coil domain. EMP2 and HSBP2 accumulate differentially during maize development and heat stress. Previous analyses revealed that EMP2 is required for regulation of *heat shock protein* (*hsp*) gene expression and also for embryo morphogenesis. Developmentally abnormal emp2 mutant embryos are aborted during early embryogenesis. To analyze EMP2 function during postembryonic stages, plants mosaic for sectors of emp2 mutant tissue were constructed. Clonal sectors of emp2 mutant tissue revealed multiple defects during maize vegetative shoot development, but these sector phenotypes are not correlated with aberrant *hsp* gene regulation. Furthermore, equivalent phenotypes are observed in emp2 sectored plants grown under heat stress and nonstress conditions. Thus, the function of EMP2 during regulation of the heat stress response can be separated from its role in plant development. The discovery of emp2 mutant phenotypes in postembryonic shoots reveals that the duplicate genes *emp2* and *hsbp2* encode nonredundant functions throughout maize development. Distinct developmental phenotypes correlated with the developmental timing, position, and tissue layer of emp2 mutant sectors, suggesting that EMP2 has evolved diverse developmental functions in the maize shoot.

EMPTY PERICARP2 (EMP2) of maize is a small, evolutionarily conserved protein composed solely of a central coiled-coil domain (Fu *et al.* 2002). Consisting of two to five amphipathic α-helices that are twisted to form a super coil, the coiled-coil motif is a dominant feature in many protein::protein interactions (Burkhard *et al.* 2001; Yu 2002). EMP2 homologous proteins are found throughout the eukaryotic domain and were first identified in humans as the HEAT SHOCK FACTOR BINDING PROTEIN1 (HSBP1) via binding interactions with HEAT SHOCK FACTOR1 (HSF1) protein (Satyal *et al.* 1998; Fu *et al.* 2002; Tai *et al.* 2002). HSF1 is a transcription factor that induces the expression of a wide range of *heat shock protein* genes (*hsp*) during thermal stress (Wiederrecht *et al.* 1988; Pirkkala *et al.* 2001). This heat-induced, upregulated transcription of *hsp*'s and other chaperonins is termed the heat shock transcriptional response (HSTR) and is likewise an extraordinarily conserved phenomenon in nature (Lindquist 1986; Gurley and Key 1991; Morimoto 1998). Previous analyses in humans and *Caenorhabditis elegans* suggest that HSBP1 binds to and inactivates animal HSF1 during attenuation of the heat shock response (Satyal *et al.* 1998). These studies suggest that the coiled-coil domain of HSBP1 plays an integral role during mediation of protein::protein interaction with animal HSF1, although no mutant phenotype is observed in null mutations of *hsbp1* in *C. elegans* (Satyal *et al.* 1998; Tai *et al.* 2002).

Two HSBP homologs are present in maize: EMP2 and HSBP2. Preliminary investigations of EMP2 suggest a conserved function in HSTR regulation during maize embryogenesis (Fu *et al.* 2002). Loss-of-function emp2 mutants exhibit early staged embryo abortion. The developmental timing of emp2 embryo lethality correlates with the initial competency of maize embryos to invoke the HSTR and with overexpression of *hsp* transcripts. However, emp2 mutant embryos display aberrant morphology throughout their abbreviated development, well before *hsp* overexpression and prior to embryonic abortion. Thus, an additional developmental function(s) of EMP2 is implied, outside of its role in HSTR regulation.

In this report, we demonstrate that the accumulation of the maize paralogues EMP2 and HSBP2 is differentially regulated in embryos and leaves. To investigate whether the paralogues function nonredundantly during postembryonic maize development, clonal sectors of emp2 mutant tissue were generated in developing maize shoots against a heterozygous nonmutant back-

Sequence data from this article have been deposited with the EMBL/GenBank Data Libraries under accession no. AY450672.

[1]*Corresponding author:* Plant Biology Department, 4615 Miller Plant Sciences Bldg., University of Georgia, Athens, GA 30602.
E-mail: mjscanlo@plantbio.uga.edu

ground. In contrast to the phenotype seen in emp2 mutant embryos, EMP2 is not required for normal regulation of *hsp* gene expression in leaves. Furthermore, numerous developmental mutant phenotypes correlate with emp2 mutant sectors in the maize vegetative shoot. Thus, this clonal sector analysis has successfully separated the function of EMP2 in HSTR regulation from its unrelated function(s) during maize shoot development. These data suggest that the EMP2 coiled-coil motif has been recruited to mediate additional protein::protein interaction(s) during the evolution of maize shoot development and that EMP2 and HSBP2 perform nonredundant functions during postembryonic as well as embryonic development.

MATERIALS AND METHODS

Maize transcript analyses: Total RNA from maize tissue was prepared by Trizol lysis buffer (GIBCO BRL, Bethesda, MD) according to the manufacturer's recommendation. Total RNA concentrations were quantified by spectrophotometry. For use in Northern gel blots, 5 μg of total RNA was loaded in each lane. Gene-specific probes for an 18-kD maize *hsp* expressed sequence tag (EST) contig (plant GDB *Zmtuc03-08-11.14919*) were PCR amplified using the primer pair: 5′-CAT CAC AAA GCT CCA AAC CCA GCA-3′ and 5′-GCC CAA GAC CAT CGA GAT TAA GGT-3′. A 0.7-kb *Eco*RI-*Xho*I digestion fragment of *Zmhsp101* cDNA (gift from D. Gallie, University of California-Riverside) was used as a gene-specific probe.

Antibody production, recombinant protein expression, immunoblot analysis, and immunolocalization: Soluble proteins from maize tissues were prepared as described previously (Fu *et al.* 2002). Recombinant proteins of EMP2 and HSBP2 were expressed separately in the pTriplEx vector (CLONTECH, Palo Alto, CA) and in the pBAD TOPO TA vector (Invitrogen, Carlsbad, CA) according to the manufacturers' recommendations. Bacterial protein preparation, protein gel electrophoresis, transfer, and Coomassie blue staining (brilliant blue R350) were performed according to standard methods (Sambrook and Russel 2001). Thirty micrograms of total protein was loaded per lane.

Rabbit anti-EMP2 (described in Fu *et al.* 2002) and anti-HSBP2 specific polyclonal antibodies were produced and affinity purified by BioSource (Camarillo, CA). The specificities of the purified antibodies were assayed by ELISA and Western gel blotting against unique multiple antigenic peptides and recombinant proteins of HSBP2. The dilutions used for primary antibodies in Western gel blot assays were 1/3000 (anti-EMP2) and 1/2000 (anti-HSBP2). Fixation, paraffin embedment, sectioning, and immunolocalization of EMP2 antigen in maize kernels were carried out as described by Sylvester and Ruzin (1994). The affinity-purified anti-EMP2 polyclonal antibodies were used as the primary antibodies at 1/100 dilution; the secondary antibodies were either goat anti-rabbit IgG-AP conjugated at 1/500 dilution (Promega, Madison, WI) or fluorescein isothiocyanate-conjugated goat anti-rabbit antibody at 1/30 dilution (Jackson ImmunoResearch, West Grove, PA). The images were obtained using a Zeiss Axioplan II equipped with a Southern Micro Instruments (Pompano Beach, FL) CCD camera.

Genetic stocks, sector generation, stress treatment, and analyses: Maize stocks heterozygous for the *emp2-R* (reference allele; Scanlon and Freeling 1997; Fu *et al.* 2002; previous designation *emp2-1047*, Scanlon *et al.* 1994) in coupling with the albino mutation *w3* were obtained by crossing plants of the genotypes *W3, Emp2/W3, emp2-R* × *w3, Emp2/W3, Emp2.* One-quarter of the kernels obtained from this cross will be *w3, Emp2/ W3, emp2-R.* Plants of this genotype were identified by the segregation of both white and emp mutant kernels on self-pollinated ears; these plants were also outcrossed to B73. The progeny were subjected to an additional round of self-pollination and outcrossing to identify individual plants that harbored the *emp2* and *w3* mutations in coupling. Outcross progeny of the *w3, emp2-R* heterozygous mutant parents were utilized for clonal analyses. All white sectored plants utilized in this report were analyzed by genomic PCR (Fu *et al.* 2002) to verify that they harbored the *emp2-R* mutation.

A total of 9000 seeds were imbibed overnight, germinated for 2 days, and subsequently irradiated at 1250–1500 rads utilizing cobalt 60 and average energy 1.25 MeV. Following radiation, 6000 seedlings were field planted, 2000 seedlings were grown at 25° in the greenhouse, and an additional 1000 seedlings were subjected to daily heat stress treatments (36° or 42° for 2 hr).

Single-leaf sectors appeared on juvenile leaves only and were harvested before plant maturity. In contrast, multiple-leaf sectors were harvested at plant maturity. All sectored plants were genotyped by PCR. Hemizygous, *w3, emp2/−* sectored plants were analyzed to determine the tissue layers occupied by the sectors; phenotypes were scanned, photographed, or photocopied as described (Scanlon 2000).

The position and width of each leaf sector was recorded relative to the lateral vein number at which the sector started and how many lateral veins the sector spanned relative to the number of total lateral veins contained within the half leaf. The lateral vein data were used to extrapolate positions of sectors on mature leaves back to the leaf primordium (Figure 1B), because lateral veins are evenly spaced in young primordia (Sharman 1942). When mixed cell layer sectors were encountered, only the sector portion that occupied the full L2-derived layer was mapped in Figure 7. For those cases wherein a narrow leaf phenotype was associated with a sector, the vein number on the nonphenotypic side of the leaf was used as the total vein number. Leaf primordia were assumed to be uniform in size, comprising 40 units in length from midrib to margin (Figure 1B). The overall distribution of sector positions on leaf primordia is presented as overlaying solid lines, with their positions and lengths correlated to the location and width of each sector. Consequently, a two-dimensional plot was derived to describe the correlation of narrow leaf phenotypes with the lateral location of sectors extrapolated to the leaf primordium.

The methodology used to extrapolate meristematic leaf sectors onto the circumference of the shoot apical meristem (SAM) is essentially the same as described previously (Figure 1; Scanlon 2000). The only modification is that the half circumference of the SAM is represented by a solid straight bar of 40 units in width, with 0 and 40 anchored for the midrib and marginal flanks of the SAM. For example, if 5 cm in girth stem contains a sector that initiates 1.5 cm away from the midrib and extends 0.5 cm laterally, the sector is represented by a solid line extending from position 24 to position 32 in Figure 8. Sectored leaves were categorized according to developmental stage (middle and adult) according to the same criteria described in Scanlon (2000).

Heat treatment of maize plants: Plants used for transcript analysis of *emp2, hsbp2,* and various maize *hsp*'s (*hsp101, hsp18, hsp82, hsp70, dnaj,* and two additional small *hsp*'s identified from maize ESTs; http://www.plantgdb.org/) were grown continuously under 25° and then heat shifted to either 36° or 42° for 2 hr, followed by recovery at 25°. Sectors and adjacent unsectored tissues were periodically sampled for analysis of

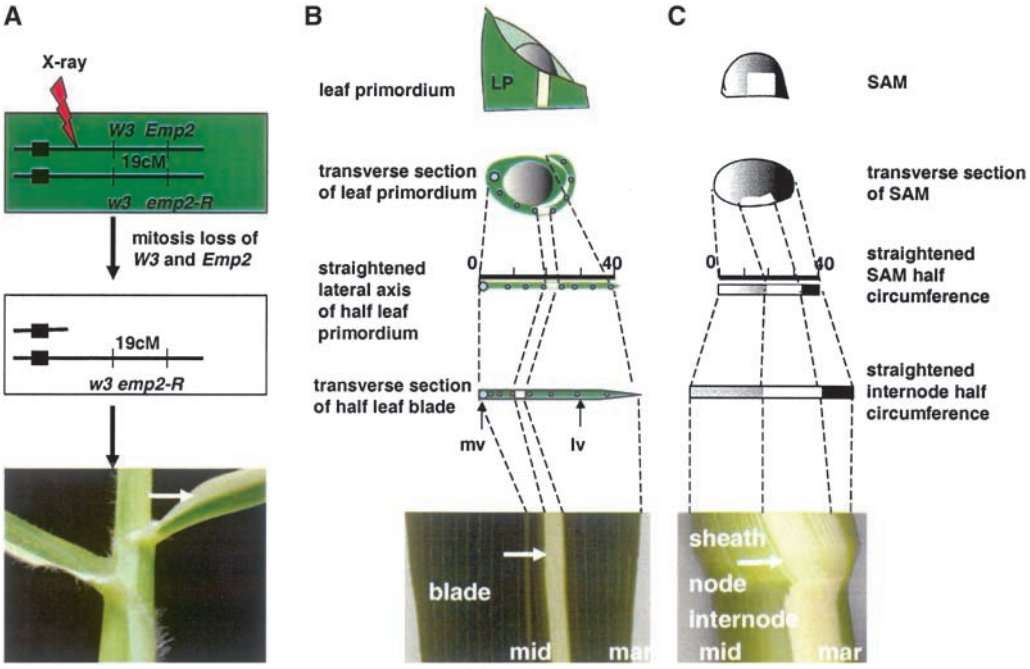

FIGURE 1.—Generation and analyses of albino-marked emp2 hemizygous sectors. (A) Schematic of a maize cell (top) heterozygous for the *emp2-R* and *w3* mutations in coupling on chromosome 2 (solid rectangles, centromere). X-ray-induced random chromosome breakage of the nonmutant chromosome proximal to the *W3* locus leads to clonal loss of the nonmutant *W3* and *Emp2* alleles in albino progeny cells (middle). Thus, sectors of albino tissue mark the clonal loss of EMP2 function (bottom). (B) Methodology used to estimate the position of emp2 mutant sectors on leaf primordia (top) via extrapolation of the sector position on mature leaves (bottom). As described in MATERIALS AND METHODS, the lateral axis of a half-leaf primordium (LP) was graphically subdivided into 40 equal increments; these increments were later correlated to the positions of lateral veins (lv) counted on the mature, sectored leaf. (C) Methodology used to estimate the lateral position of sectors within the SAM via extrapolation of the position of sectors within the internode of mature plants. See MATERIALS AND METHODS for further details. mid, midrib domain; mar, margin; mv, midvein.

maize *hsp* transcripts by Northern gel blot analyses as described in FU *et al.* (2002).

RESULTS

The homologous proteins EMP2 and HSBP2 show differential accumulation in maize embryos and leaves: RT-PCR and Northern gel blot analyses revealed that *emp2* and *hsbp2* are both expressed constitutively in all tissues examined. However, Western analyses using gene product-specific antibodies (see MATERIALS AND METHODS) indicate that the EMP2 and HSBP2 proteins accumulate differentially in maize embryos and leaves (Figure 2). Specifically, EMP2 protein is more abundant in 16-day-after-pollination (DAP) embryos than in mature leaves, whereas HSBP2 protein is less abundant in embryos than in leaves. Also, whereas EMP2 protein levels are not heat inducible in leaves, accumulation of HSBP2 protein is induced in the maize leaf following incubation for 2 hr at 36° and 42° (Figure 2).

Immunohistolocalization analyses reveal that EMP2 protein accumulates in the nuclei and, to a lesser extent, in the cytoplasm of maize embryonic cells (Figure 3E). No tissue-specific localization of EMP2 protein is observed; equivalent levels of protein are detected in all embryonic cell types, including the scutellum, and organs of the root and shoot pole. In addition, longitudinal and transverse sectioning of maize embryos revealed no compartmentalized accumulation of EMP2 proteins within the SAM or in leaf primordia (Figure 3, B–D).

Analyses of EMP2 function in the postembryonic shoot: generation of EMP2 loss-of-function clonal sectors: The embryo lethality of the homozygous emp2 mutants precludes traditional genetic analyses of EMP2 function in the postembryonic shoot. To study the function of EMP2 beyond embryogenesis, a clonal mosaic analysis was performed in which the *emp2-R* mutation was exposed in hemizygous, albino-marked sectors (*w3*, *emp2-R/−*, *−*) in a nonmutant (*w3*, *emp2-R/W3*, *Emp2*)

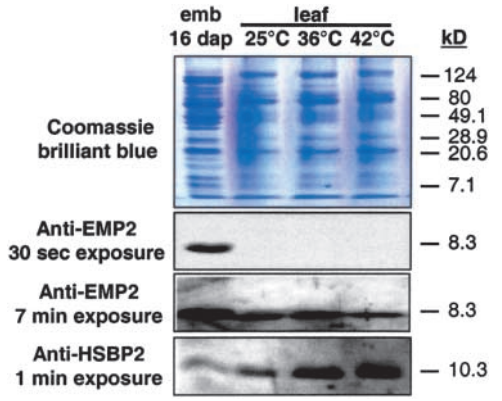

FIGURE 2.—EMP2 and HSBP2 show differential accumulation and responses to heat stress. Western gel blot analyses reveal that EMP2 protein preferentially accumulates in 16-DAP embryos (emb) and is not heat inducible in mature leaves. In contrast, the paralogue HSBP2 preferentially accumulates in leaves rather than in embryos, and accumulation of HSBP2 is induced following heat treatment of leaves.

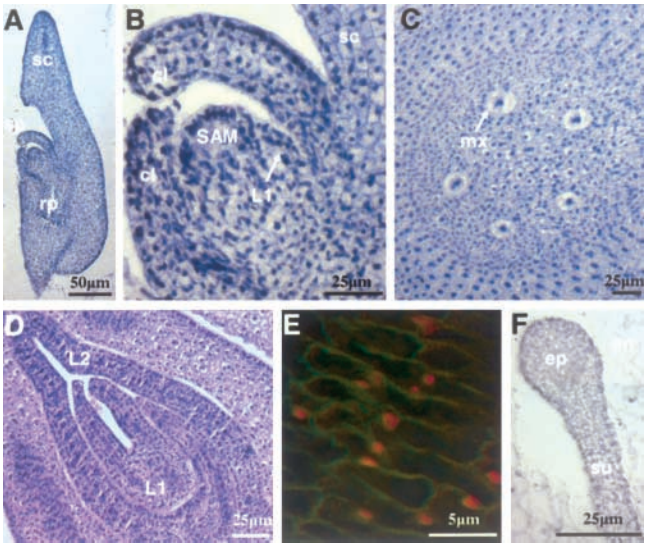

Figure 3.—Tissue and cellular localization of EMP2 protein. (A) Immunohistolocalization of EMP2 protein in maize embryos. Longitudinal section of a maize 14-DAP embryo reveals accumulation of EMP2 protein (dark blue) throughout the embryo, including the scutellum (sc), shoot pole (sp), and root pole (rp). (B) Close-up of the shoot pole of the embryo shown in A reveals equivalent accumulation of EMP2 protein in the SAM, coleoptile (cl), leaf primordium (L1), and scutellum (sc). Transverse sections of the root (C) and shoot (D) of a 24-DAP maize embryo show even accumulation of EMP2 proteins throughout the lateral axes of the embryo. (E) Merged UV fluorescence/light micrograph analyses of subcellular localization of EMP2 protein (red) in 14-DAP pericarp cells reveal accumulation predominately in the nucleus although faint signals are detected outside the nucleus. Cell walls autofluoresce green. (F) 12-DAP emp2 null mutant embryo does not accumulate EMP2 protein. ep, embryo proper; en, endosperm; su, suspensor.

genetic background by X-ray-induced random chromosome breakage proximal to the *W3* locus (Figure 1). Previous mosaic analyses utilizing the *w3* albino marker confirmed that aside from albinism, hemizygous clonal sectors of w3 mutant leaf tissue do not alone cause disturbances in shoot morphological development (Foster *et al.* 1999; Scanlon 2000). Therefore, developmental abnormalities associated with albino emp2 null mutant sectors enable phenotypic analyses of EMP2 function(s) in adult maize shoots. The cell autonomy, organ/tissue layer specificity, and developmental timing of EMP2 function in the shoot may also be inferred from clonal analysis.

Western gel blot analyses confirmed that no EMP2 protein is detectable in emp2 null albino sectors, although EMP2 does accumulate in sectors hemizygous for the nonmutant *Emp2* allele (Figure 4). These data reveal that the *emp2-R* allele is a null mutation in maize leaves as well as in embryo, although the paralogous protein HSBP2 accumulated to equivalent levels in both emp2 null and nonmutant albino sectors (data not shown).

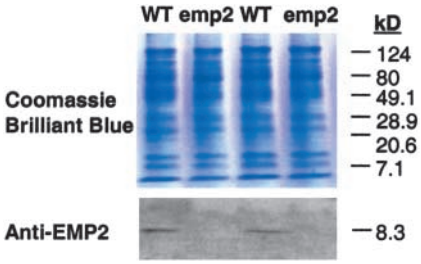

Figure 4.—The emp2/− mutant sectors do not accumulate EMP2 protein. Western gel blot analyses reveal that EMP2 protein accumulated in the sectors that are hemizygous for the nonmutant *Emp2* allele (WT), but not in *emp2-R* hemizygous sectors (emp2).

Therefore, the accumulation of EMP2 and HSBP2 is not coregulated in maize leaves.

Expression of *hsp* genes is unaffected within emp2 mutant leaf sectors: To decipher whether EMP2 regulates *hsp* expression in the postembryonic shoot (as it does in maize embryos; Fu *et al.* 2002), transcript levels of seven different maize *hsp*'s (including *hsp101, hsp18, hsp82, hsp70, dnaj,* and two additional small *hsp*'s identified as ESTs; Vierling *et al.* 1989; Marrs *et al.* 1993; Lund *et al.* 1998; Young *et al.* 2001; Nieto-Sotelo *et al.* 2002) were analyzed via RNA gel blots before, during, and after heat stress in both mutant sectored and adjacent wild-type unsectored leaf tissues. Sectors of emp2 mutant tissue had no effect on the accumulation of any of the *hsp* transcripts analyzed; the data for *hsp101* and *hsp18* are shown in Figure 5. When grown at nonstress temperatures (25°), transcripts of *hsp101* and *hsp18* in emp2 null sectors and in adjacent unsectored tissues are not detected (Figure 5). However, after plants were heat shocked at 42° for 2 hr, accumulation of *hsp* gene transcripts was induced equivalently in both unsectored and emp2 null sectored leaf tissues. Notably, restoration of nonstress temperature corresponded with the prompt (within 2 hr) attenuation of *hsp* transcription in both

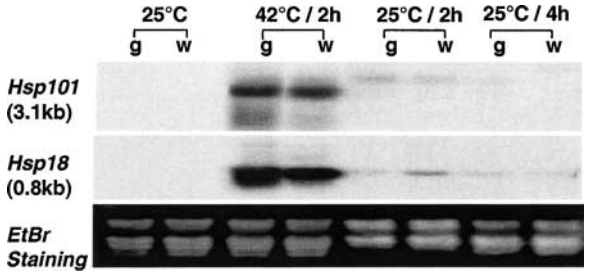

Figure 5.—The accumulation of maize heat shock protein transcripts is unaffected in sectors of emp2 null mutant leaf tissue. RNA gel blot analyses of emp2 null sectored (w) and adjacent, nonmutant unsectored leaf tissue (g) reveal equivalent accumulation of both *hsp101* and *hsp18* transcripts before (25°), during (42°), and after (25°/2 hr and 25°/4 hr) heat stress.

TABLE 1

emp2 mutant sectors and phenotypes

Phenotypes (no. of affected leaves)	Sector timing		Sector tissue layer				
	Meristematic	Nonmeristematic	L2 alone	L1–L2	Adaxial L2[a]	Internal L2 alone	Abaxial L2[a]
Ligule/auricle displacement (11)	2	9	6	3	2	0	0
Abnormal phyllotaxy (8)	12[b]	0	2	7	3[c]	0	3[c]
Narrow leaf (28)	14[d]	9	12	17	0	0	0
Narrow leaf with accessory leaf	4	0	4	0	0	0	0
Narrow leaf with lobe growth	2	0	0	2	0	0	0
No phenotype (141)[e]	8	45	34	28	13	2	11
Total sectored leaves (188)[e]	32[f,g]	63	52[f]	53[g]	18	2	14

[a] Includes sectors extended into the internal L2 layer.
[b] The 12 meristematic sectors condition 8 abnormal phyllotaxy leaves.
[c] Both the adaxial and abaxial L2 are sectored but not the internal layer.
[d] The 14 meristematic sectors condition 20 narrow leaves.
[e] Not all the emp2 mutant sectors on leaves have their tissue layer and developmental timing determined.
[f] Sectors 77 and 89 were associated with both narrow leaf phenotypes and abnormal phyllotaxy.
[g] Sectors 96 and 97 were associated with both narrow leaf phenotypes and abnormal phyllotaxy.

emp2 null sectored and nonmutant leaf tissue (Figure 5). Thus, whereas EMP2 is required for correct *hsp* gene regulation in maize embryos (Fu *et al.* 2002), this function of EMP2 is dispensable in maize leaves. As elaborated below, these analyses have successfully separated the *hsp* gene regulatory function of EMP2 from its role in plant development.

Clonal sectors of loss of EMP2 function in the maize shoot correlate with diverse developmental defects: To investigate the function(s) of EMP2 during postembryonic shoot development, a total of 117 sectored plants (encompassing 245 leaves) of >6000 irradiated seedlings were examined. Among them, 98 sectors (encompassing 188 total leaves) were genotyped as *emp2-R/−* via PCR analysis, while the remaining sectors were *Emp2/−*. No developmental phenotype was observed in any hemizygous sectors from *Emp2/Emp2* plants (data not shown), while 48 of the emp2/− sectors were associated with developmental defects (Tables 1–5, Figure 6). As described above (Figure 5), none of the emp2-R/− null albino sectors showed aberrant *hsp* gene expression at ambient temperature, during heat shock, or after recovery from heat shock. Moreover, equivalent developmental phenotypes were observed in field-grown emp2 sectored plants, in plants grown in the greenhouse under non-heat shock conditions (<25°), as well as in plants grown in the greenhouse subjected to heat stress treatment (2 hr/day at 36° or 42° as described in MATERIALS AND METHODS). Therefore, the emp2 sector phenotypes appear to be unrelated to heat shock or the heat shock response and reflect additional functions of EMP2 during postembryonic shoot development.

The mutant phenotypes were summarized into three major classes in Table 1: displaced ligule/auricle structure (Table 2; Figure 6A), abnormal leaf phyllotaxy (Table 3; Figure 6D), and narrow leaves (Table 4; Figure 6, E–K). As detailed below, the expression of particular mutant phenotypes was correlated with distinct spatial and temporal patterns of emp2/− null sector induction.

Ligule/auricle displacement sectors: Grass leaves contain a distal blade and a proximal sheath, which are separated by the ligule/auricle structures (SHARMAN 1941). The ligule is an epidermis-derived elaboration of fringe-like tissue on the adaxial leaf surface of the sheath/blade boundary. The auricle is a V-shaped structure that initiates from two points on either side of the midrib and expands outward toward each margin (SYLVESTER *et al.* 1990). Development of the ligule and auricle is temporally correlated and genetically inseparable (HARPER and FREELING 1996).

There were 11 emp2 null sectors traversing the ligule and auricle that disrupted the continuity of these structures (Figure 6A). Specifically, the ligule/auricle was interrupted at the boundary between the midrib side of nonmutant tissue and the mutant sectored tissue, but it was continuous across the marginal side boundary of the sector. A second ligule/auricle initiated *de novo* on the midrib side boundary of the mutant sector. The newly initiated ligule/auricle was always displaced proximal to the original auricle and extended laterally to the leaf margin. Although sectors of *liguleless1* (*lg1*) mutation also caused proximal displacement of the ligule/auricle structure, the displacement occurred on the nonmutant tissue lying marginal to the sectored mutant tissue (BECRAFT and FREELING 1991). Within the *lg1* mutant sectored tissue the ligule/auricle structure was completely removed (BECRAFT *et al.* 1990).

As shown in Tables 1 and 2, ligule/auricle displace-

TABLE 2

Ligule/auricle emp2 sectors

Sector no. (leaf no.)[a]	Sector type[b]	Leaf stage[c]	Lateral vein no.	Sector position[d]	Tissue layer[e]	Phenotype[f]
23 (3)	Nonmeristematic	J	L6, R6	R4-4.5	wwwww	Y
24 (3)	Nonmeristematic	J	L6, R6	L2-2	wwwww	Y
25 (3)	Nonmeristematic	J	L6, R6	R3-4	wwwww	Y
30 (4)	Nonmeristematic	J	L8, R8	L1-1.5	GwwGG	Y
37 (4)	Nonmeristematic	J	L9, R9	L3-5	GwwGG	Y
46 (3)	Nonmeristematic	J	L8, R8	L3-3.5	GwwwG	Y
52 (6)	Nonmeristematic	J	L13, R10	L1.5-2	GwwwG	Y
56 (4)	Nonmeristematic	J	L12, R12	R2-3	GwwwG	Y
59 (5)	Nonmeristematic	J	L9, R10	R7-E	GwwwG	Y
65 (14)	Meristematic	A	L18, R18	ND	ND	N
65 (15)	Meristematic	A	L18, R18	L4-4.1	GwwwG	Y
91 (11)	Meristematic	M	L22, R22	ND	ND	N
91 (12)	Meristematic	M	L22, R22	R10.5-12	GwwwG	Y

[a] For plants harvested at maturity, six basal leaves were assumed to be lost.
[b] Sectors spanning more than one phytomer were categorized as meristematic while those restricted in a single phytomer were recognized as nonmeristematic.
[c] Leaf stages were categorized as juvenile leaf (J, leaves 1–8), middle-stage leaf (M, leaves 9–13), and adult-stage leaf (A, leaf 14 and beyond).
[d] The sector position relative to midvein is denoted as follows: L, left side of midvein; R, right side of midvein; E, leaf edge; and ND, not determined.
[e] The transverse dimension of the leaf is divided into five designated layers: adaxial L1 derived, adaxial L2 derived, middle L2 derived, abaxial L2 derived, and abaxial L1 derived. w, white emp2 null tissue; G, green nonmutant tissue; ND, not determined.
[f] N, there is no ligule/auricle displacement phenotype; Y, there is ligule/auricle displacement phenotype.

ment phenotypes are associated with both meristematic and nonmeristematic *emp2-R/−* hemizygous sectors. Although the majority of ligule/auricle sectors (9 of 11) extended through all L2-derived tissue layers (Figure 6B) of the leaf, 2 of the ligule sectors occupied only the adaxial L2-derived leaf tissues (Figure 6C). These data suggest that the correct proximodistal positioning of the adaxial ligule/auricle requires EMP2 function in L2-derived adaxial leaf tissues.

Abnormal phyllotaxy sectors: Maize leaves initiate in an alternate phyllotaxy; successive leaves arise ~180° apart and offset in two ranks. However, eight cases of abnormal phyllotaxy were observed in emp2 mutant sectored plants, in which successive nodes were not located on opposite sides of the stem. The degree of deviation from the 180° divergence angle varied among different sectored plants. These included cases wherein two successive leaves arose on the same side of the plant; in extreme cases two leaves arose from a single node. In the example shown in Figure 6D (Table 3, sectors 66 and 67) only one of these leaves (L14) contained a midrib, and both leaves are arranged in an abnormal phyllotaxy with respect to the previous leaf. In all cases in which a leaf arose in an abnormal phyllotactic pattern, either the affected leaf *or* the previous leaf contained two, separate *emp2-R/−* sectors located on opposite sides of the midvein (Table 3; Figure 6D). These data indicate that the sectors that generated phyllotaxy phenotypes were present at or prior to the founder cell stage of leaf development. Finally, although the majority of these phenotypes arose from sectors marking all L2-derived tissue layers, two partial L2-derived sectors also conferred this phenotype (Table 1). These partial L2-derived sectors reveal that EMP2 function is required in *all* cells throughout the meristematic L2 tissue layer to establish normal leaf phyllotaxy.

Narrow leaf sector phenotypes: Plant leaves are composed of at least two mediolateral zones: a central domain, which includes the midrib and leaf tip, and a lateral domain that includes the lower leaf margins. In this clonal analysis, we observed 28 cases of lateral leaf domain deletion phenotypes (Table 1). The *emp2-R* mutation may correlate with either complete deletion of the lateral leaf domain (*i.e.*, comprising the blade and sheath; 17 cases) or partial deletion of the lateral leaf domain (*i.e.*, comprising the blade alone or blade plus distal sheath; 11 cases).

Representatives of the complete lateral domain deletion phenotypes are depicted in Figure 6, E and F. As shown in Figure 6E, the sheath and proximal blade of the emp2/− null sectored half leaf are much narrower and contain fewer lateral veins than do the unsectored counterparts. Nonmutant leaf blade margins develop distinctive sawtooth hairs and a nonchlorophyllic, tapered edge (Figure 6H), whereas transverse sections of the emp2/− sectored narrow leaf margins revealed blunted, chlorophyllic leaf edges and the absence of sawtooth margin hairs (Figure 6G). Margin structures were normal, however, in sectored regions of the upper leaf blade. These observations are consistent with previ-

TABLE 3

Abnormal phyllotaxy emp2 mutant sectors

Sector no. (leaf no.)[a]	Sector type[b]	Leaf stage[c]	Lateral vein no.	Sector position[d]	Tissue layer[e]	Phenotype[f]
67 (11)	Meristematic	M	L18, R18	R(0.2-0.8)	wwwww	N
67:66 (12)	Meristematic	M	L22, R22	L(14-16.5) R(13-E)	wwwww	N
66:67 (13)	Meristematic	M	ND	L(0-0.8) R(1.5-2.5)	wwwww	N
67:66 (14)	Meristematic	M	L21, R22 (SL31)	R(14-16) R(9.5-10.5)	wwwww	Y
76 (7)	Meristematic	J	L7, R14	L(5-6.5)	wwwww	N
76 (8)	Meristematic	J	L12, R12	R(4-6)	wwwww	N
76:77 (9)	Meristematic	M	L17, R13	L(3.5-4.5) R(13-13)	wwwww	N
77:76 (10)	Meristematic	M	L19, R19	L(4-4.5) R(5-7.5)	wwwww	Y
85:84 (13)	Meristematic	M	L22, R22	L(5-6.5) R(6.5-10)	wwwww	Y
89:89 (13)	Meristematic	M	L20, R23	L(12.5-E) R(ND)	wwwww	Y
93:94 (14)	Meristematic	M-A	L17, R17	L(2-7.5) R(14.5-E)	GwGwG	Y
95:94 (15)	Meristematic	A	L16, R16	L(0-1) R(6.5-8.5)	GwGwG	Y
96 (11)	Meristematic	M	L18, R14	L(14-14)	GwwwG	N
96 (12)	Meristematic	M	L20, R20	R(0.3-0.7)	GwwwG	N
96 (13)	Meristematic	M	L20, R20	L(ND)	GwwwG	N
97:96 (14)	Meristematic	A	L13, R20	L(13-13) R(0.5-1.5)	GwwwG	Y
96:97 (15)	Meristematic	A	AL16, L9, R18	AL(8-16) L(9-9) R(3-4)	GwwwG	Y
97 (16)	Meristematic	A	L17, R9	L(1-E)	GwwwG	N
97 (17)	Meristematic	A	L11, R14	R(6.5-E)	GwwwG	N

[a] For plants harvested at maturity, six basal leaves were assumed to be lost.

[b] Sectors were categorized as meristematic sectors and nonmeristematic sectors as described in MATERIALS AND METHODS.

[c] Leaf stages were categorized as juvenile leaf (J, leaves 1–8), middle-stage leaf (M, leaves 9–13), and adult-stage leaf (A, leaf 14 and beyond).

[d] The sector position relative to midvein is denoted as follows: L, left side of midvein; R, right side of midvein; E, leaf edge; SL, secondary leaf; and AL, accessory leaf. SL is an independent leaf whereas AL designates an elaborated accessory leaf domain that is fused to a narrow leaf. When a sector starts and ends with the same lateral vein, this sectored lateral vein abuts leaf edge.

[e] Transverse dimension of leaf is divided into five layers: adaxial L1, adaxial L2, middle L2, abaxial L2, and abaxial L1. w, white emp2 null tissue; G, green nonmutant tissue; ND, not determined.

[f] N, there is no abnormal phyllotaxy phenotype; Y, there is abnormal phyllotaxy phenotype.

ous reports (SCANLON *et al.* 1996) demonstrating that margins of the upper leaf are derived from a different leaf compartment (*i.e.*, the central domain) than are margins of the lower leaf.

The emp2 null albino sectors also gave rise to less severe narrow leaf phenotypes in which the sectored side of the leaf contained fewer lateral veins, yet developed normal margin structures. The sectored sheath either was unaffected or contained a partial deletion that was constrained to the distal sheath region. Furthermore, four sectored narrow leaves were each attached to an accessory leaf (Figure 6J); fusion of the narrow leaf to the accessory leaf occurred in the sheath epidermis (data not shown). The accessory leaves were composed of either sheath plus blade or sheath alone and were positioned immediately adjacent to the corresponding narrow leaf on the node. The accessory leaf phenotype was associated with only meristematic emp2/− null sectors marking the L2-, but not the L1-derived layers (Tables 1 and 4). In addition, two sectored narrow leaves were associated with abnormal outgrowths of sheath tissue that contained highly branched, reticulated, and discontinuous vasculature near the blade sheath boundary of the leaf (Figure 6K). The sheath outgrowth phenotypes correlated with complete L1–L2 layered sectors.

The 28 cases of narrow leaf phenotypes were associated with a total of 23 emp2 null sectors. Only meristematic sectors and nonmeristematic sectors that extended into both sheath and blade conferred narrow leaf phenotypes (Tables 1 and 4). This suggests that EMP2 function is required prior to the completion of early leaf primordial development, after which time these proximal-distal leaf compartments become clonally distinct (POETHIG and SZYMKOWIACK 1995). In addition, all narrow leaf sectors displayed fully albino internal (L2-derived) tissue layers, suggesting that the EMP2 function in a subset of L2-derived tissues is enough for the elaboration of the lateral leaf domain. Finally, although the majority of narrow leaf sectors were astride the abnormal leaf edge (Figure 6E), some sectors were internal to the margin (Figure 6, F and G).

The expression of narrow leaf phenotypes correlates with the lateral position of emp2 null albino sectors: Although immunohistolocalization analyses of developing maize shoots reveal equivalent accumulation of EMP2 protein throughout all maize tissues examined (Figure 3), a correlation between sector position and the narrow leaf phenotype suggested a compartmentalized function(s) of EMP2. To identify the location of this putative EMP2 functional domain, the lateral positions

TABLE 4

Narrow leaf emp2 sectors

Sector no. (leaf no.)[a]	Sector type[b]	Leaf stage[c]	No. of lateral vein	Sector position (vein)[d]	Internode girth	Sector position (internode)[d]	Tissue layer[e]	Phenotype[f]
1 (5)	Nonmeristematic	J	L8, R4	R 3-4	ND	ND	GwwwG	Narrow
44 (5)	Nonmeristematic	J	L12, R9	R 3.5-4	ND	ND	GwwwG	Narrow
47 (4)	Nonmeristematic	J	L9, R8	R 7-E	ND	ND	wwwww	Partial
51 (3)	Nonmeristematic	J	L10, R7	R 6-E	ND	ND	wwwww	Narrow
53 (6)	Nonmeristematic	J	L13, R10	R 4-4	ND	ND	GwwwG	Narrow
55 (5)	Nonmeristematic	J	L13, R10	R 5.5-6	ND	ND	GwwwG	Narrow
58 (5)	Nonmeristematic	J	L10, R8	R 8-E	ND	ND	wwwww	Partial
62 (3)	Nonmeristematic	J	L7, R9	L 5-6	ND	ND	GwwwG	Partial
64 (5)	Nonmeristematic	J	L9, R13	L 7-E	ND	ND	wwwww	Narrow
68 (10)	Meristematic	M	L20, R17	R 8.5-E	8.8	R 2.4-3.5	GwwwG	Narrow
68 (9)	Meristematic	M	L17, R17	L 3-3.5	ND	ND	GwwGG	N
70 (11)	Meristematic	M	L17, R23	L 14-E	7.1	L 3.0-3.2	wwwww	Partial
70 (12)	Meristematic	M	L23, R23	R 1.5-2.5	8.2	R 0.6-0.8	wwwww	N
70 (13)	Meristematic	M	L17, R25	L 13-E	7.0	L 2.5-3.0	wwwww	Partial
70 (14)	Meristematic	A	L21, R21	R 1.5-2.5	ND	ND	wwwww	N
70 (15)	Meristematic	A	L20, R20	L 13-15	5.8	L 2.2-2.3	wwwww	N
72 (13)	Meristematic	M	L22, R19	L (ND)	4.7	L 2.0-2.2	wwwww	Partial
72 (14)	Meristematic	A	L17, R19	R 0.5-1	4.0	R 1.0-1.1	wwwww	N
72 (11)	Meristematic	M	L13, R19	L 12.5-E	5.5	L 2.2-2.3	GwwwG	Narrow, AL
72 (12)	Meristematic	M	L22, R22	R 0-0.5	ND	ND	wwwww	N
73 (12)	Meristematic	M	L22, R19	L (ND)	4.7	L 1.1-1.4	wwwww	N
73 (13)	Meristematic	M-A	L17, R19	R 5.5-15	4.0	R 1.5-1.6	wwwww	Partial
73 (11)	Meristematic	M	L22, R22	R 5-7.5	5.3	R 1.2-1.3	wwwww	N
74 (12)	Meristematic	M	L19, R19	L 1-2	ND	ND	wwwww	N
74 (13)	Meristematic	M-A	L19, R17	R 13.5-E	4.5	R 1.6-1.9	wwwww	Partial
74 (14)	Meristematic	A	L13, R13	R 10.5-E	ND	ND	GwwwG	N
75 (8)	Meristematic	J	L7, R14	L 7-E	ND	ND	wwwww	Narrow, AV
77 (11)	Meristematic	M	L17, R13	R 13-13	5.9	R 1.5-2.5	wwwww	Narrow
77 (12)	Meristematic	M	L19, R19	L 5-7.5	5.5	L 1.5-1.6	wwwww	N
77 (13)	Meristematic	M	L20, R20	L 5-7.5	ND	ND	wwwww	N
82 (11)	Meristematic	M	L16, R16	R 11-11.5	ND	ND	wwwww	N
82 (13)	Meristematic	M	L17, R19	L 11-E	ND	ND	wwwww	Narrow
83 (11)	Meristematic	M	L22, R22	R 0.5-1	6.0	R 0.1-0.2	GwwwG	N
83 (12)	Meristematic	M	L12, R22	L 12-12	ND	ND	wwwww	Narrow, AV
83 (14)	Meristematic	A	L18, R18	L 15-E	4.1	L 1.9-2.0	GwwwG	N
89 (13)	Meristematic	M-A	L20, R23	L12.5-E	4.3	L 1.6-2.1	wwwww	Partial
92 (13)	Meristematic	M	ND	R1.5-2	ND	ND	wwwww	N
92 (14)	Meristematic	M-A	L15, R19	L12-E	ND	ND	wwwww	Partial
96 (11)	Meristematic	M	L14, R18	L14-14	ND	ND	wwwww	Partial
96 (12)	Meristematic	M	L20, R20	R 0.3-0.7	6	R 0.1-0.2	GwwwG	N
96 (13)	Meristematic	M	L20, R20	L (ND)	6	L 2.8-3.0	GwwwG	N
96 (14)	Meristematic	A	L13, R20	R 0.5-1.5	5.5	R 0.1-0.3	GwwwG	N
96 (15)	Meristematic	A	(AL16) L9, R18	AL 8-16, L 9-9	4.6	R 1.6-2.3	GwwwG	Narrow, AL
97 (14)	Meristematic	A	L13, R20	L 13-13	ND	ND	GwwwG	Narrow
97 (15)	Meristematic	A	(AL16) L9, R18	R 3-4	4.6	R 0.3-0.4	GwwwG	N
97 (16)	Meristematic	A	L17, R9	R1-E	4.0	R 0.3-1.1	GwwwG	Narrow, AL
97 (17)	Meristematic	A	L11, R14	L6.5-E	3.5	L 1.0-1.4	GwwwG	Narrow
98 (12)	Meristematic	M	L17, R17	L (ND)	3.2	L 0.3-0.6	GwwwG	N
98 (13)	Meristematic	M	L17, R7	R (ND)	3.3	R 1.0-1.2	GwwwG	N
98 (14)	Meristematic	A	L13, R13	L (ND)	2.8	L 0.45-0.6	GwwwG	N
98 (15)	Meristematic	A	L12, R12	R (ND)	2.4	R 0.5-0.6	GwwwG	N
98 (16)	Meristematic	A	L10, R10	L (ND)	2.0	L 0.30-0.5	GwwwG	N
98 (17)	Meristematic	A	L9, R7	R (ND)	2.0	R 0.5-1.2	GwwwG	Narrow, AL

[a] For plants harvested at maturity, six basal leaves were assumed to be lost.

[b] Sectors spanning more than one phytomer were categorized as meristematic while those restricted in a single phytomer were recognized as nonmeristematic.

[c] Leaf stages were categorized as juvenile leaf (J, leaves 1–8), middle-stage leaf (M, leaves 9–13), and adult-stage leaf (A, leaf 14 and beyond).

[d] The sector position relative to the midvein is denoted as follows: L, left side of midvein; R, right side of midvein; E, leaf edge; AL, accessory leaf; and ND, not determined.

[e] The transverse dimension of the maize leaf is divided into five layers: adaxial L1, adaxial L2, middle L2, abaxial L2, and abaxial L1. w, white emp2 null tissue; G, green nonmutant tissue; ND, not determined.

[f] N, no narrow leaf phenotype; narrow, narrow leaf in both sheath and blade; np, narrow leaf only in the blade and upper sheath; AL, accessory leaf; AV, abnormal vasculature.

TABLE 5

Nonphenotypic emp2 sectors

Sector no. (leaf no.)[a]	Sector type[b]	Leaf stage[c]	Lateral vein no.	Sector position[d]	Tissue layer[e]
2 (5)	Nonmeristematic	J	L8, R8	L6-6.5	GwwGG
3 (6)	Nonmeristematic	J	L12, R12	L5-7	GwwwG
4 (4)	Nonmeristematic	J	L10, R10	R6.5-7.5	wwwww
5 (5)	Nonmeristematic	J	L10, R10	L0-0.5	GGwwG
6 (6)	Nonmeristematic	J	ND	R0-1	GwwGG
7 (6)	Nonmeristematic	J	L10, R10	R6-8	GwwwG
8 (3)	Nonmeristematic	J	L6, R6	L2-3	GGwGG
10 (4)	Nonmeristematic	J	L8, R5	L1-2[f]	GwGGG
11 (5)	Nonmeristematic	J	L9, R9	L6.5-7	GwGwG
12 (4)	Nonmeristematic	J	L9, R9	R5-6	GwwwG
13 (5)	Nonmeristematic	J	L9, R9	R6-8	GwwwG
14 (4)	Nonmeristematic	J	L6, R7	R1-2[f]	GGGwG
15 (5)	Nonmeristematic	J	L10, R10	L4-5	GwGGG
16 (4)	Nonmeristematic	J	L8, R8	R7-E	GwwwG
17 (3)	Nonmeristematic	J	L12, R12	R10.5-E	wwwww
18 (5)	Nonmeristematic	J	L9, R9	L4-5	wwwww
19 (5)	Nonmeristematic	J	L9, R9	L7.2-7.8	GwwwG
20 (5)	Nonmeristematic	J	L10, R10	R6.5-7	GwwwG
21 (4)	Nonmeristematic	J	L7, R7	L5-5.5	GGwGG
22 (4)	Nonmeristematic	J	L9, R9	L6-7	GwwGG
26 (4)	Nonmeristematic	J	L8, R8	R4-5	GGGwG
27 (4)	Nonmeristematic	J	L10, R10	L1-1.8	GwwGG
28 (4)	Nonmeristematic	J	L9, R9	R5.5-6.5	GwwwG
29 (4)	Nonmeristematic	J	L8, R8	L3-4	GwwGG
31 (3)	Nonmeristematic	J	L7, R7	R2-2.5	GwwwG
32 (3)	Nonmeristematic	J	L7, R7	L4-4.5	GwGwG
33 (4)	Nonmeristematic	J	L8, R8	L5-6	wwwww
34 (5)	Nonmeristematic	J	L10, R10	L4-4.5	GwwwG
35 (4)	Nonmeristematic	J	L11, R11	L2-3	GwwwG
36 (5)	Nonmeristematic	J	L12, R12	R8-9	GGGww
38 (4)	Nonmeristematic	J	L9, R9	L3-4	GwGGG
39 (4)	Nonmeristematic	J	L9, R9	R7-7.5	GGGwG
40 (3)	Nonmeristematic	J	L7, R7	R6-7	GwwwG
41 (3)	Nonmeristematic	J	L7, R7	R3-3.5	GGwwG
42 (3)	Nonmeristematic	J	L8, R8	R5-5.5	GwwwG
43 (5)	Nonmeristematic	J	L12, R9	L1-1.5[f]	GwwwG
48 (5)	Nonmeristematic	J	L10, R10	R4.5-5	GGGwG
49 (6)	Nonmeristematic	J	L10, R10	L8.5-E	wwwww
54 (5)	Nonmeristematic	J	L13, R10	L5-5.5[f]	GwwGG
57 (2)	Nonmeristematic	J	L7, R7	R3-3.5	GwwwG
60 (2)	Nonmeristematic	J	L8, R8	R4.5-5	GwGGG
61 (4)	Nonmeristematic	J	L10, R10	L5,7	GGGwG
63 (5)	Nonmeristematic	J	L9, R13	R2-2.5[f]	GwwwG
71 (10)	Meristematic	M	L13, R19	R13-14.5[f]	wwwww
78 (12)	Meristematic	M	L19, R19	L4-4.5	wwwww
80 (10)	Meristematic	M	L19, R19	L8-8.5	wwwGw
80 (11)	Meristematic	M	L21, R21	R7-7.5	wwwGw
81 (11)	Meristematic	M	L21, R21	R3-4.5	GwwwG
86 (12)	Meristematic	M	L23, R23	R11-12.5	wwwww
86 (13)	Meristematic	M	L23, R23	L3-4	wwwww
87 (11)	Meristematic	M	L22, R22	L10-12	GwwwG
87 (13)	Meristematic	M	L21, R21	R9.5-11.5	GwGwG
88 (11)	Meristematic	M	L22, R22	R9.5-10.5	GwwwG
88 (12)	Meristematic	M	L22, R22	ND	ND
90 (11)	Meristematic	M	L22, R22	L3-4	GwwwG
90 (12)	Meristematic	M	L22, R22	R7.5-8.5	GwwwG

[a] For plants harvested at maturity, six basal leaves were assumed to be lost.

[b] Sectors spanning more than one phytomer were categorized as meristematic while those restricted in a single phytomer were recognized as nonmeristematic.

[c] Leaf stages were categorized as juvenile leaf (J, leaves 1–8) and middle-stage leaf (M, leaves 9–13).

[d] The sector position relative to the midvein is denoted as follows: L, left side of midvein; R, right side of midvein; E, leaf edge; and ND, not determined.

[e] Transverse dimension of leaf is divided into five layers: adaxial L1, adaxial L2, middle L2, abaxial L2, and abaxial L1. w, white emp2 null tissue; G, green nonmutant tissue; ND, not determined.

[f] Sectors on the normal side of a narrow leaf are designated as not associated with mutant phenotype.

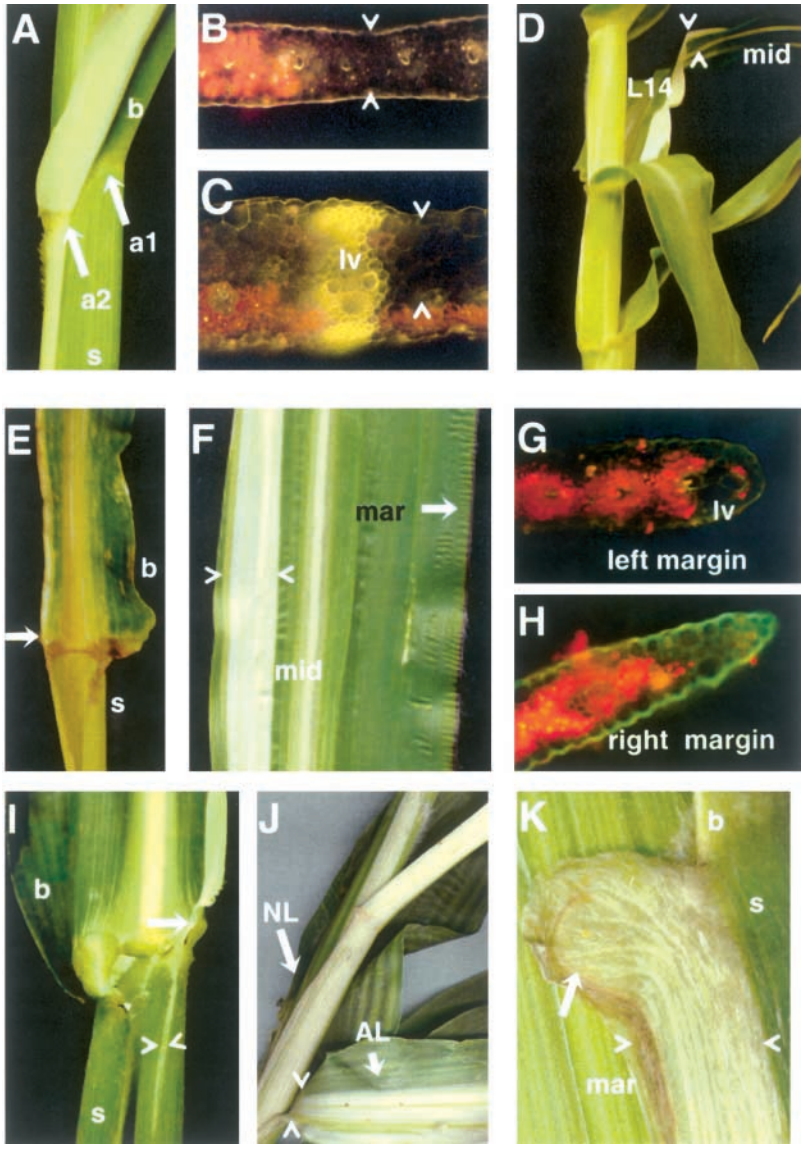

FIGURE 6.—Multiple developmental defects are associated with emp2 mutant sectors. (A) In sector 59, leaf 6, the ligule/auricle structure within the mutant sector is displaced proximally (a2, auricle) compared to the ligule/auricle structure in the unsectored portion of the leaf (a1, auricle). UV fluorescence micrographs (chlorophyll is red) reveal that ligule/auricle displacement phenotypes are associated with emp2 sectors (bordered by carets) that were contained in all L2-derived tissue layers (B) and also in sectors confined to adaxial L2-derived tissues, sector 37, leaf 4 (C). (D) In sectors 66 and 67, leaf 14, abnormal phyllotaxy of emp2 sectored leaves is seen. Two leaves arose from the same node and in dechussate phyllotaxy, as opposed to the alternate phyllotaxy of adjacent leaves. Note that leaf 14 (L14) contains two independent emp2 sectors (carets) straddling the midrib. (E and F) In sector 51, leaf 3, and sector 82, leaf 13, emp2 mutant sectors lead to the deletion of a lateral leaf domain (arrow) in both the sheath (s) and the blade (b). UV fluorescence micrograph of the left margin of the narrow leaf blade shown in F is blunted and chlorophyllic (G), whereas the nonmutant right margin of the same leaf (H) is tapered and nonchlorophyllic. (I) Sector 96, leaf 11 shows a partial narrow leaf emp2 mutant sector (carets) in which the lateral domain deletion is localized to the leaf blade and the upper part of sheath only. (J) Sector 97, leaf 16 shows a narrow leaf emp2 sector in which an accessory leaf (AL, arrow) is attached to a narrow leaf (NL, arrow). (K) Sector 83, leaf 12 shows an emp2 mutant sector in which an abnormal outgrowth of sheath tissue is hypervascularized and the normal parallel vascular pattern is disrupted. b, blade; s, sheath; mid, midrib; mar, margin; lv, lateral vein.

of narrow leaf phenotypic and nonphenotypic *emp2/−* null sectors were compared. However, the nonuniform, postprimordial expansion of different regions of the maize leaf precluded direct comparison of sector positions within mature leaves (STEFFENSON 1968; POETHIG 1986). Therefore, the sector locations were compared using lateral veins as a reference for sector positioning (Figure 7; SCANLON and FREELING 1997; see MATERIALS AND METHODS). Lateral veins are established and evenly spaced during early stages of maize leaf development (SHARMAN 1942; BOSABALIDIS *et al.* 1994) and thus are good indicators of sector position within young leaf primordia. As shown in Figure 7A, the vast majority (24/28) of narrow leaf mutant sectors were contained on the marginal half of the mutant leaf; this region is termed the emp2 phenotypic domain. The clustering of phenotypes within the emp2 phenotypic domain reveals a localized EMP2 function, instead of uneven distribution of emp2 null sectors (Figure 7B).

The fact that not all sectors located within the emp2 phenotypic domain conditioned mutant phenotypes suggests that additional factors, such as the timing of sector induction (Table 1), are important for the expression of narrow leaf phenotypes. For example, whereas all meristematic emp2 null sectors within this domain yielded narrow leaf phenotypes, many postmeristematic sectors did not. In addition, the exact location of EMP2 function is not fixed from meristem to meristem, as discussed below. The mapped location of the emp2 phenotypic domain prompted us to investigate whether EMP2 functions within the lateral meristem domain, a region whose boundaries are marked by foci of NARROW SHEATH (NS) function and expression (SCANLON 2000; NARDMANN *et al.* 2004). Correspondingly, the emp2 null phenotypic domain was also mapped onto the shoot meristem by determining the meristematic positions of phenotypic and nonphenotypic multiple-leaf sectors (see MATERIALS AND METHODS). As shown in Figure 8, all multiple-leaf sectors associated with narrow leaf phenotypes were localized to the emp2 phenotypic domain,

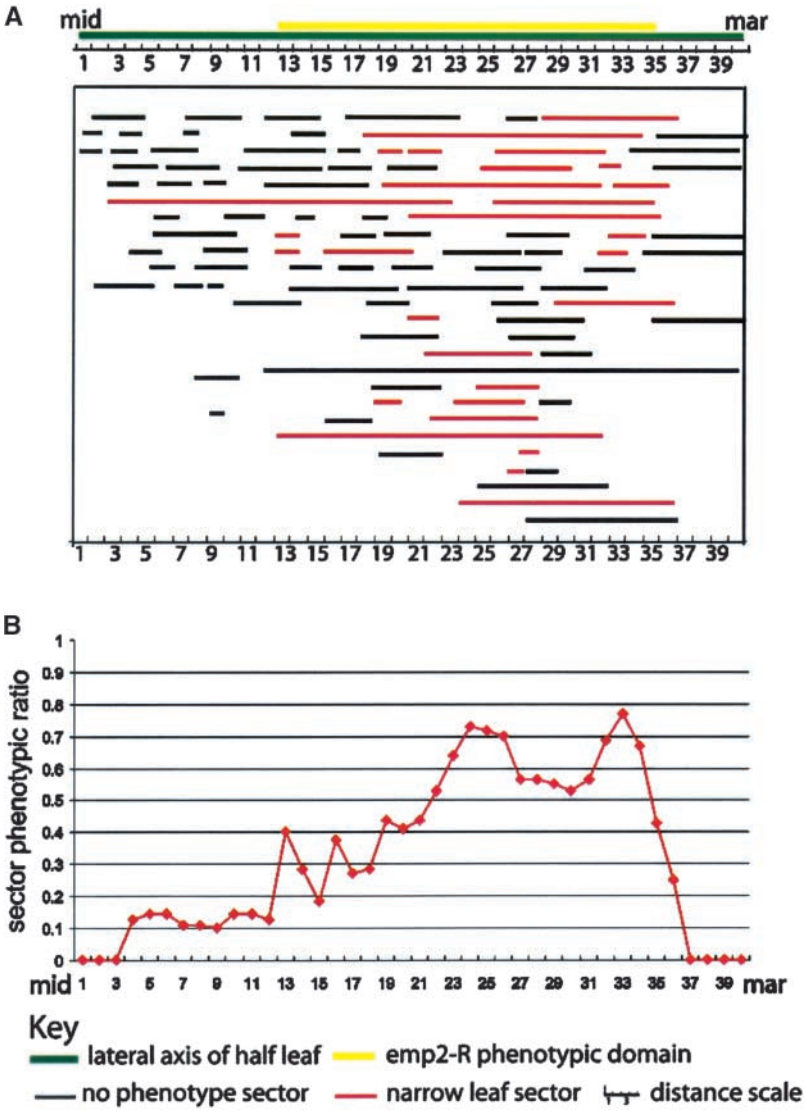

FIGURE 7.—The narrow leaf phenotypic emp2 mutant sectors are clustered in the marginal half of the maize leaf. (A) The positions of 91 emp2 mutant leaf sectors occupying all L2-derived leaf tissues were extrapolated to the lateral axis of the half-leaf primordium using the lateral veins as described in Figure 1 and MATERIALS AND METHODS. The emp2 null phenotypic domain (yellow bar) is defined as the region of a leaf primordium, as measured by percentage of total lateral veins within which narrow leaf phenotypic sectors are observed. (B) The sector phenotypic ratio represents the percentage of total emp2 mutant sectors in a given mediolateral domain that conditioned narrow leaf sector phenotypes.

whereas nonphenotypic sectors were all restricted from this region. Interestingly, the emp2 null phenotypic domain overlaps with and extends beyond the NS foci. As the meristem proceeds from middle to adult stages of vegetative development the position of the emp2 null phenotypic domain recedes laterally toward the midrib; a similar phenomenon was observed for the NS foci (SCANLON 2000). It was also noted that the severity of the narrow leaf phenotype correlates with the lateral position of the emp2 null albino sector. That is, emp2 null sectors within the NS foci were mainly associated with a complete lateral domain deletion phenotype (Figures 6, E and F, and 8). In contrast, sectors within the emp2 phenotypic domain, but outside the NS focus, caused only partial domain deletion phenotypes (Figures 6I and 8).

DISCUSSION

The maize HSBP proteins have evolved divergent functions: Previously we reported that *hsbp* orthologs were duplicated prior to the speciation of monocot grasses (FU *et al.* 2002). Herein we demonstrate that the products of the duplicated maize *hsbp* genes, *emp2* and *hsbp2*, accumulate differently during development and stress response. The differential protein accumulation patterns suggest divergent functions for the maize paralogous proteins. Previous emp2 mutant analyses suggested a role for EMP2 in regulating the HSTR in maize embryos, whereas the heat-induced accumulation of the maize HSBP2 protein suggests that HSBP2 carries out this function in maize leaves. In this model, the heat-induced accumulation of HSBP2 protein may bind to and inactivate maize HSFs and consequently attenuates the HSTR. Mutant analysis of *hsbp2* will enable tests of this hypothesis.

Although EMP2 seems to not have an essential role in regulating the HSTR in maize leaves, it does have important, nonredundant functions during maize shoot development. As reported above, a diverse array of developmental defects associate with the sectored loss of EMP2 function in maize shoots, whereas all nonmutant

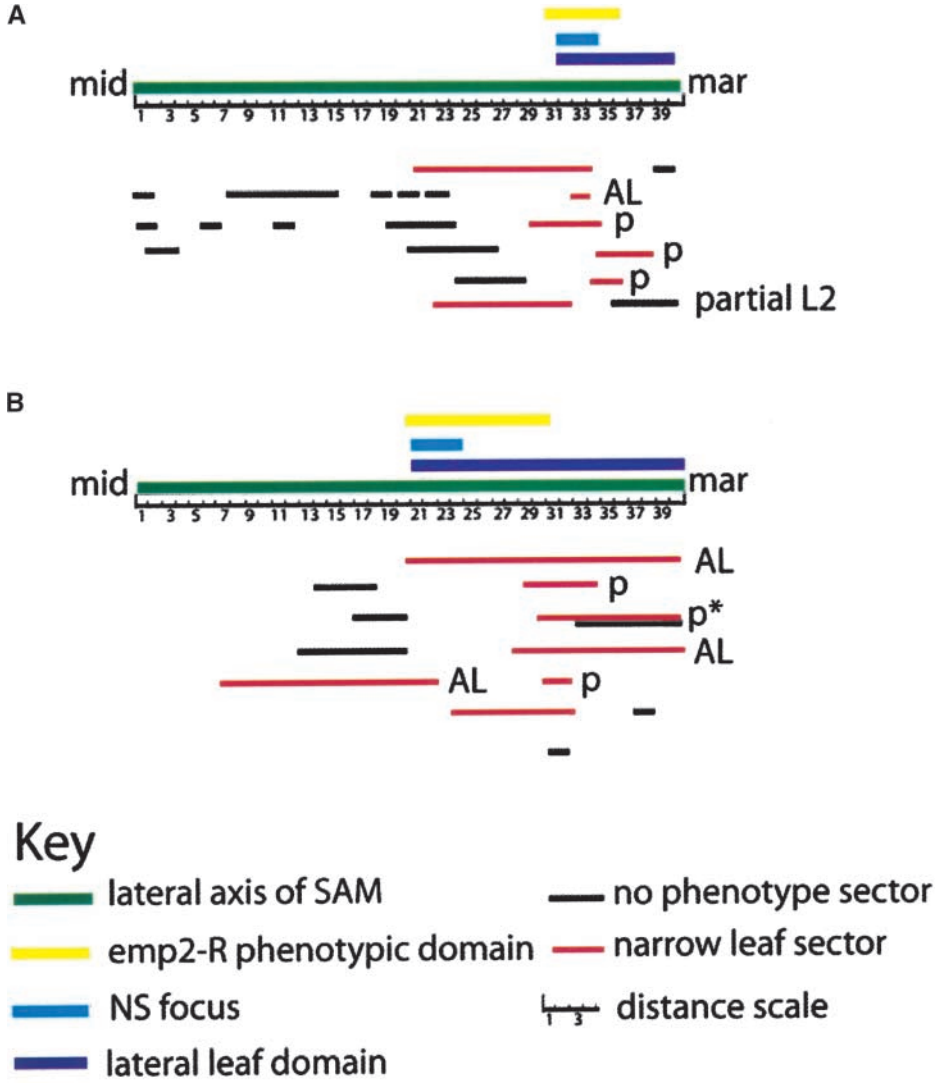

FIGURE 8.—Meristematic sectors reveal that the emp2 null phenotypic domain is localized to lateral leaf domains. Sector locations on the SAM were estimated by extrapolation of the lateral position of sectors on the internode, as described in Figure 1 and MATERIALS AND METHODS. The emp2 null phenotypic domain (yellow bar) is defined as described above. (A) Phenotypic sectors (red lines) marking middle-staged leaves (leaves 9–13) are localized to the emp2 null phenotypic domain (yellow bar). (B) This emp2 null phenotypic domain maps to a focus located relatively closer to the midrib in adult-staged leaves (leaf 14 and above). Sectors in which an accessory leaf was attached are indicated. The NS focus (blue bar) demarcates midrib side boundary of the lateral leaf domain (purple bar; SCANLON 2000). Asterisk denotes a broad sector that covers both leaf margins in which only one margin is abnormal. p, partial lateral leaf domain deletion; AL, accessory leaf.

Emp2/− sectors included in our analysis were nonphenotypic. Previous mosaic analyses with the *w3* allele also demonstrated that albinism, as well as hemizygosity for most of chromosome arm 2L, does not condition these observed developmental defects in maize shoots (FOSTER *et al.* 1999; SCANLON 2000). Thus, these phenotypes were specifically linked to the *emp2-R* mutation.

Heat stress treatment at specific developmental stages is known to induce diverse developmental defects in Drosophila (MITCHELL and LIPPS 1978; PETERSEN and MITCHELL 1987). Likewise, the aberrant expression of *hsp90* caused dwarfism, radial symmetrical leaves, and missing leaves in Arabidopsis (QUEITSCH *et al.* 2002). The requirement of EMP2 during regulation of *hsp* gene expression in maize embryos initially led to the hypothesis that the range of emp2/− null sector phenotypes observed in this study resulted from aberrant *hsp* expression: corn plants in the field are often heat stressed and the emp2 null sectors may not be able to attenuate the HSTR. However, EMP2 is not required to regulate the heat shock response in young leaves (Figure 5), nor did we detect aberrant expression of non-heat-inducible *hsp*'s in emp2 null sectors (data not shown). More importantly, we found that the growth temperature and stress treatment of the sectored plants did not affect the range of phenotypes conferred by the emp2 null sectors (data not shown). Therefore, the developmental defects in *emp2/−* null sectored plants are not caused by a defective heat shock response, suggesting that additional functions of EMP2 are involved in the observed mutant phenotypes. Taken together, genetic and molecular analyses presented herein successfully demonstrated the functional divergence of the maize paralogous proteins EMP2 and HSBP2. EMP2 has evolved additional functions, which are distinct from its conserved function in regulating the HSTR.

Distinct functions of EMP2 during maize shoot development: Sectored loss of EMP2 function in the postembryonic shoot can lead to the deletion of a leaf domain, displacement of the ligule and auricle, or altered phyllotaxy (Figure 6). One possible explanation of these results is that the tissue loss and tissue/organ displacement

phenotypes are caused by a generalized emp2 mutant defect that causes cell death or lack of cell proliferation in sectored tissues. However, several features of the emp2 mutant sectors fail to support this hypothesis. For example, there is no evidence of cell death associated with emp2 null sectored shoot tissue. In contrast, the emp2 null sectored tissues are expansive and morphologically healthy (Figure 6). In addition, the number of cell files between sectored lateral veins is equivalent to that observed in adjoining, nonsectored tissues (Figure 6, B, G, and H, and data not shown). These data are especially informative because lateral veins in maize are established during early primordial stages (Sharman 1942), such that a defect in cell proliferation would be manifested as a reduction in intervein spacing. Thus, the sector data strongly suggest that EMP2 is not required for general cell proliferation or viability in the postembryonic maize shoot, although it may be important for proliferation of some specific cell types. It is also possible that the emp2/− null sectors retard the competency of cells to respond to developmental cues at the appropriate time.

The particular phenotype of any emp2/− null sector is correlated with the developmental timing, lateral positioning, and tissue layer specificity of the mutant sector (Table 1). For example, the altered phyllotaxy phenotype was observed only in cases wherein two separate, L2-derived, meristematic emp2 null sectors straddled the midrib-forming region. Current models of phyllotaxy determination inspired by surgical excision of leaf primordia (reviewed in Snow and Snow 1933; Wardlaw 1949; Steeves and Sussex 1989), auxin manipulation of the SAM (Reinhardt *et al.* 1998, 2000, 2003; Vernoux *et al.* 2000), and the phyllotaxy mutation *terminal ear1* (Veit *et al.* 1998) suggest that existing leaf primordia generate an inhibitory signal(s) to prevent premature leaf initiation. The sector data presented herein suggest that EMP2 is somehow required in the shoot meristem to initiate, propagate, or otherwise respond to this leaf inhibitory signal. Furthermore, the presence of EMP2 protein within any portion of L2-derived tissue on just one flank of the meristem is sufficient to maintain this inhibitory signal and normal phyllotaxy. In another example, previous analyses revealed that the leaf lateral domain is patterned in the shoot meristem by a non-cell-autonomous recruitment function initiating at the NS lateral foci (Scanlon 2000). Likewise, sectored loss of EMP2 function within the emp2 phenotypic domain also correlates with the complete or partial deletion of a lateral leaf region. These data suggest that EMP2 function in the meristem and early leaf primordium is also required for the elaboration of the lateral leaf domain.

We suggest that these emp2 null sector phenotypes are due to the loss of expanded (*i.e.*, non-HSTR-related) functions of the EMP2 coiled-coil domain in the maize shoot. The coiled coil is a common protein motif in nature, and specific coiled-coil domain proteins have been shown to interact with multiple, unrelated protein pairing partners that function in disparate molecular pathways (reviewed in Burkhard *et al.* 2001; Newman and Keating 2003). Currently, we are utilizing yeast two-hybrid and proteomic approaches to investigate the distinct protein::protein interactions of EMP2 and HSBP2 in maize embryos and shoots. Preliminary results suggest that these maize HSBP paralogues do indeed interact differently with maize HSF isoforms and other maize proteins (S. Fu, unpublished results). Perhaps the identification of EMP2 interacting proteins will help dissect the molecular pathways governing maize developmental processes such as ligule/auricle positioning, lateral leaf development, and phyllotaxy.

We thank K. Dawe, L. Pratt, R. Meagher, and Z.-H. Ye for helpful discussions throughout this work and A. Tull and M. Boyd of the Plant Biology Greenhouses for expert care of maize plants. We thank D. Gallie and T. Young from the University of California-Riverside for the maize hsp101 cDNA plasmids. We are grateful for the assistance of M. Crenshaw and J. Parker (Athens Regional Medical Center) and J. E. Noakes (Center for Applied Isotope Studies) in irradiation of maize seedlings. We thank K. Dawe, J. Ji, and reviewers from Genetics for critical evaluation of the manuscript. The work was funded by U.S. Department of Agriculture-COOP State Research Education and Extension Service-National Research Initiative Competitive Grants Program grant 01-01600 to M.S.

LITERATURE CITED

Becraft, P. W., and M. Freeling, 1991 Sectors of liguleless-1 tissue interrupt an inductive signal during maize leaf development. Plant Cell **3:** 801–807.

Becraft, P. W., D. K. Bongard-Pierce, A. W. Sylvester, R. S. Poethig and M. Freeling, 1990 The *liguleless-1* gene acts tissue specifically in maize leaf development. Dev. Biol. **141:** 220–232.

Bosabalidis, A. M., R. F. Evert and W. A. Russin, 1994 Ontogeny of the vascular bundles and contiguous tissues in the maize leaf blade. Am. J. Bot. **81:** 745–752.

Burkhard, P., J. Stetefeld and S. V. Strelkov, 2001 Coiled coils: a highly versatile protein folding motif. Trends Cell Biol. **11:** 82–88.

Foster, T., B. Veit and S. Hake, 1999 Mosaic analysis of the dominant mutant, Gnarley1-R, reveals distinct lateral and transverse signaling pathways during maize leaf development. Development **126:** 305–313.

Fu, S., R. Meeley and M. J. Scanlon, 2002 *Empty pericarp2* encodes a negative regulator of the heat shock response and is required for maize embryogenesis. Plant Cell **14:** 3119–3132.

Gurley, W. B., and J. L. Key, 1991 Transcriptional regulation of the heat-shock response: a plant perspective. Biochemistry **30:** 1–12.

Harper, L., and M. Freeling, 1996 Interactions of *liguleless1* and *liguleless2* function during ligule induction in maize. Genetics **144:** 1871–1882.

Lindquist, S., 1986 The heat-shock response. Annu. Rev. Biochem. **55:** 1151–1191.

Lund, A. A., P. H. Blum, D. Bhattramakki and T. E. Elthon, 1998 Heat-stress response of maize mitochondria. Plant Physiol. **116:** 1097–1110.

Marrs, K. A., E. S. Casey, S. A. Capitant, R. A. Bouchard, P. S. Dietrich *et al.*, 1993 Characterization of two maize HSP90 heat shock protein genes: expression during heat shock, embryogenesis, and pollen development. Dev. Genet. **14:** 27–41.

Mitchell, H. K., and L. S. Lipps, 1978 Heat shock and phenocopy induction in Drosophila. Cell **15:** 907–918.

Morimoto, R. I., 1998 Regulation of the heat shock transcriptional response: cross talk between a family of heat shock factors, molec-

ular chaperones, and negative regulators. Genes Dev. **12:** 3788–3796.

Nardmann, J., J. Ji, W. Werr and M. J. Scanlon, 2004 The maize duplicate genes *narrow sheath1* and *narrow sheath2* encode a conserved homeobox gene function in a lateral domain of shoot apical meristems. Development **131:** 2827–2839.

Newman, J. R., and A. E. Keating, 2003 Comprehensive identification of human bZIP interactions with coiled-coil arrays. Science **300:** 2097–2101.

Nieto-Sotelo, J., L. M. Martinez, G. Ponce, G. I. Cassab, A. Alagon *et al.*, 2002 Maize HSP101 plays important roles in both induced and basal thermotolerance and primary root growth. Plant Cell **14:** 1621–1633.

Petersen, N. S., and H. K. Mitchell, 1987 The induction of a multiple wing hair phenocopy by heat shock in mutant heterozygotes. Dev. Biol. **121:** 335–341.

Pirkkala, L., P. Nykanen and L. Sistonen, 2001 Roles of the heat shock transcription factors in regulation of the heat shock response and beyond. FASEB J. **15:** 1118–1131.

Poethig, R. S., 1989 Genetic mosaics and cell lineage analysis in plants. Trends Genet. **5:** 273–277.

Poethig, R. S., and E. J. Szymkowiack, 1995 Clonal analysis of leaf development in maize. Maydica **40:** 67–76.

Queitsch, C., T. A. Sangster and S. Lindquist, 2002 Hsp90 as a capacitor of phenotypic variation. Nature **417:** 618–624.

Reinhardt, D., F. Wittwer, T. Mandel and C. Kuhlemeier, 1998 Localized upregulation of a new expansin gene predicts the site of leaf formation in the tomato meristem. Plant Cell **10:** 1427–1437.

Reinhardt, D., T. Mandel and C. Kuhlemeier, 2000 Auxin regulates the initiation and radial position of plant lateral organs. Plant Cell **12:** 507–518.

Reinhardt, D., E. R. Pesce, P. Stieger, T. Mandel, K. Baltensperger *et al.*, 2003 Regulation of phyllotaxis by polar auxin transport. Nature **426:** 255–260.

Sambrook, J., and D. W. Russel, 2001 *Molecular Cloning: A Laboratory Manual*, Ed. 3. Cold Spring Harbor Laboratory Press, Cold Spring Harbor, NY.

Satyal, S. H., D. Chen, S. G. Fox, J. M. Kramer and R. I. Morimoto, 1998 Negative regulation of the heat shock transcriptional response by HSBP1. Genes Dev. **12:** 1962–1974.

Scanlon, M. J., 2000 NARROW SHEATH1 functions from two meristematic foci during founder-cell recruitment in maize leaf development. Development **127:** 4573–4585.

Scanlon, M. J., and M. Freeling, 1997 Clonal sectors reveal that a specific meristematic domain is not utilized in the maize mutant narrow sheath. Dev. Biol. **182:** 52–66.

Scanlon, M. J., P. S. Stinard, M. G. James, A. M. Myers and D. S. Robertson, 1994 Genetic analysis of 63 mutations affecting maize kernel development isolated from Mutator stocks. Genetics **136:** 281–294.

Scanlon, M. J., R. G. Schneeberger and M. Freeling, 1996 The maize mutant narrow sheath fails to establish leaf margin identity in a meristematic domain. Development **122:** 1683–1691.

Sharman, B. C., 1941 Development of the ligule in *Zea mays* L. Nature **147:** 641.

Sharman, B. C., 1942 Developmental anatomy of the shoot of *Zea mays* L. Ann. Bot. **6:** 245–284.

Snow, M., and R. Snow, 1933 Experiments on phyllotaxis. II. The effect of displacing a primordium. Philos. Trans. R. Soc. Lond. **222:** 353–400.

Steeves, T. A., and I. M. Sussex, 1989 *Patterns in Plant Development.* Cambridge University Press, Cambridge, UK.

Steffenson, D. M., 1968 A reconstruction of cell development in the shoot apex of maize. Am. J. Bot. **55:** 354–369.

Sylvester, A. W., and S. E. Ruzin, 1994 Light microscopy. I. Dissection and microtechnique, pp. 83–94 in *The Maize Handbook*, edited by M. Freeling and V. Walbot. Springer-Verlag, New York.

Sylvester, A. W., W. Z. Cande and M. Freeling, 1990 Division and differentiation during normal and liguleless-1 maize leaf development. Development **110:** 985–1000.

Tai, L. J., S. M. McFall, K. Huang, B. Demeler, S. G. Fox *et al.*, 2002 Structure-function analysis of the heat shock factor-binding protein reveals a protein composed solely of a highly conserved and dynamic coiled-coil trimerization domain. J. Biol. Chem. **277:** 735–745.

Veit, B., S. P. Briggs, R. J. Schmidt, M. F. Yanofsky and S. Hake, 1998 Regulation of leaf initiation by the *terminal ear1* gene of maize. Nature **393:** 166–168.

Vernoux, T., J. Kronenberger, O. Grandjean, P. Laufs and J. Traas, 2000 PIN-FORMED 1 regulates cell fate at the periphery of the shoot apical meristem. Development **127:** 5157–5165.

Vierling, E., L. M. Harris and Q. Chen, 1989 The major low-molecular-weight heat shock protein in chloroplasts shows antigenic conservation among diverse higher plant species. Mol. Cell. Biol. **9:** 461–468.

Wardlaw, C. W., 1949 Experiments on organogenesis in ferns. Growth Suppl. **13:** 93–131.

Wiederrecht, G., D. Seto and C. S. Parker, 1988 Isolation of the gene encoding the S. cerevisiae heat shock transcription factor. Cell **54:** 841–853.

Young, T. E., J. Ling, C. J. Geisler-Lee, R. L. Tanguay, C. Caldwell *et al.*, 2001 Developmental and thermal regulation of the maize heat shock protein, HSP101. Plant Physiol. **127:** 777–791.

Yu, Y. B., 2002 Coiled-coils: stability, specificity, and drug delivery potential. Adv. Drug Deliv. Rev. **54:** 1113–1129.

Communicating editor: J. Birchler